



UNIVERSITÀ  
DEGLI STUDI  
FIRENZE

## FLORE

# Repository istituzionale dell'Università degli Studi di Firenze

### **HEDGEHOG-GLI Signaling Drives Self-Renewal and Tumorigenicity of Human Melanoma-Initiating Cells.**

Questa è la Versione finale referata (Post print/Accepted manuscript) della seguente pubblicazione:

*Original Citation:*

HEDGEHOG-GLI Signaling Drives Self-Renewal and Tumorigenicity of Human Melanoma-Initiating Cells / Santini R;Vinci MC;Pandolfi S;Penachioni JY;Montagnani V;Olivito B;Gattai R;Pimpinelli N;Gerlini G;Borgognoni L;Stecca B. - In: STEM CELLS. - ISSN 1066-5099. - STAMPA. - 30:(2012), pp. 1808-1818. [10.1002/stem.1160]

*Availability:*

The webpage <https://hdl.handle.net/2158/770864> of the repository was last updated on

*Published version:*

DOI: 10.1002/stem.1160

*Terms of use:*

Open Access

La pubblicazione è resa disponibile sotto le norme e i termini della licenza di deposito, secondo quanto stabilito dalla Policy per l'accesso aperto dell'Università degli Studi di Firenze (<https://www.sba.unifi.it/upload/policy-oa-2016-1.pdf>)

*Publisher copyright claim:*

La data sopra indicata si riferisce all'ultimo aggiornamento della scheda del Repository FloRe - The above-mentioned date refers to the last update of the record in the Institutional Repository FloRe

(Article begins on next page)

## HEDGEHOG-GLI Signaling Drives Self-Renewal and Tumorigenicity of Human Melanoma-Initiating Cells

ROBERTA SANTINI,<sup>a</sup> MARIA C. VINCI,<sup>a</sup> SILVIA PANDOLFI,<sup>a</sup> JUNIA Y. PENACHIONI,<sup>a</sup> VALENTINA MONTAGNANI,<sup>a</sup> BIAGIO OLIVITO,<sup>b</sup> RICCARDO GATTAI,<sup>c</sup> NICOLA PIMPINELLI,<sup>d</sup> GIANNI GERLINI,<sup>e</sup> LORENZO BORGOGNONI,<sup>e</sup> BARBARA STECCA<sup>a</sup>

<sup>a</sup>Laboratory of Tumor Cell Biology, Core Research Laboratory—Istituto Toscano Tumori (CRL-ITT), Florence, Italy;

<sup>b</sup>Department of Pediatrics, Immunology Unit, Anna Meyer Children's Hospital, Florence, Italy; <sup>c</sup>Department of Medical-Surgical Critical Area, General and Oncological Surgery, and <sup>d</sup>Department of Dermatology, University of Florence, Florence, Italy; <sup>e</sup>Plastic Surgery Unit, S.M. Annunziata Hospital—Regional Melanoma Referral Center, Istituto Toscano Tumori, Florence, Italy

**Key Words.** Cancer stem cells • Self-renewal • Signal transduction • Growth inhibition

### ABSTRACT

The question of whether cancer stem/tumor-initiating cells (CSC/TIC) exist in human melanomas has arisen in the last few years. Here, we have used nonadherent spheres and the aldehyde dehydrogenase (ALDH) enzymatic activity to enrich for CSC/TIC in a collection of human melanomas obtained from a broad spectrum of sites and stages. We find that melanomaspheres display extensive in vitro self-renewal ability and sustain tumor growth in vivo, generating human melanoma xenografts that recapitulate the phenotypic composition of the parental tumor. Melanomaspheres express high levels of Hedgehog (HH) pathway components and of embryonic pluripotent stem cell factors *SOX2*, *NANOG*, *OCT4*, and *KLF4*. We show that human melanomas contain a subset of cells expressing high ALDH activity (ALDH<sup>high</sup>), which is endowed with higher self-renewal and tumorigenic abilities than the ALDH<sup>low</sup> population. A good correlation between the

number of ALDH<sup>high</sup> cells and sphere formation efficiency was observed. Notably, both pharmacological inhibition of HH signaling by the SMOOTHENED (SMO) antagonist cyclopamine and GLI antagonist GANT61 and stable expression of shRNA targeting either SMO or GLI1 result in a significant decrease in melanoma stem cell self-renewal in vitro and a reduction in the number of ALDH<sup>high</sup> melanoma stem cells. Finally, we show that interference with the HH-GLI pathway through lentiviral-mediated silencing of SMO and GLI1 drastically diminishes tumor initiation of ALDH<sup>high</sup> melanoma stem cells. In conclusion, our data indicate an essential role of the HH-GLI1 signaling in controlling self-renewal and tumor initiation of melanoma CSC/TIC. Targeting HH-GLI1 is thus predicted to reduce the melanoma stem cell compartment. *STEM CELLS* 2012;30:1808–1818

Disclosure of potential conflicts of interest is found at the end of this article.

### INTRODUCTION

Melanoma is the most aggressive and lethal among skin cancers, known for its high metastatic potential, enhanced heterogeneity, and resistance to chemotherapy. Prognosis for patients with advanced metastatic melanoma remains poor, with a median survival time of 6–9 months and a 3-year survival rate of only 10%–15% [1]. Adjuvant therapy with IFN $\alpha$ , recommended after resection of primary melanomas with lymph node metastases, provides modest disease-

free survival [2]. The conventional drugs used for metastatic melanomas produce only transient responses [3]. Recent clinical trials using the BRAF (v-raf murine sarcoma viral oncogene homolog B1) inhibitor Vemurafenib [4] and the monoclonal antibody against CTLA-4 Ipilimumab [5] have shown better therapeutic responses, although resistance mechanisms and severe adverse effects have already been described (e.g., 6–9).

Several types of human cancer have been shown to contain a subset of cells endowed with tumorigenic potential and stem cell properties, that is the ability to self-renew and to

Author contributions: R.S. and M.C.V.: conception and design, collection and/or assembly of data, data analysis and interpretation, and final approval of manuscript; S.P., J.Y.P., V.M., and B.O.: collection and/or assembly of data and final approval of manuscript; R.G., N.P., G.G., L.B.: provision of material and final approval of manuscript; B.S.: conception and design, financial support, administrative support, data analysis and interpretation, manuscript writing, and final approval of manuscript.

Correspondence: Barbara Stecca, Ph.D., Laboratory of Tumor Cell Biology, Core Research Laboratory—Istituto Toscano Tumori (CRL-ITT), Viale Morgagni 50, 50134 Florence, Italy. Telephone: +39-055-459-8258; Fax: +39-055-459-8900; e-mail: Barbara.Stecca@ittumori.it Received January 23, 2012; Revised May 29, 2012; accepted for publication June 6, 2012; first published online in *STEM CELLS EXPRESS* June 21, 2012. © AlphaMed Press 1066-5099/2012/\$30.00/0 doi: 10.1002/stem.1160

give rise to differentiated progeny. These cells, called cancer stem cells (CSC) or tumor-initiating cells (TIC), are proposed to drive tumor initiation and progression as well as therapy resistance [10–12]. It has been suggested that CSC/TIC might exist in melanoma, but their identity and frequency are still debated [13]. Several markers have been used to prospectively isolate stem subpopulations in melanomas, including CD20, a combination of CD133 and ABCG2, ABCB5, MDR1, and CD271, or high aldehyde dehydrogenase (ALDH) activity [14–20]. However, two recent studies using a severely immunocompromised mouse model suggested high frequency of TIC in melanoma [21, 22]. These studies failed to find any correlation between a specific phenotype and tumor-initiating ability and led to questioning the existence of melanoma stem cells [21, 22]. Thus, it remains unanswered whether tumor maintenance is sustained by each individual melanoma cell or only by a distinct subpopulation of cells. In the latter scenario, the elucidation of molecular signaling driving self-renewal and tumorigenicity of CSC/TIC would be critical in order to find ways to eradicate them.

The Hedgehog-GLI (HH-GLI) pathway is an intercellular signaling playing a role in determining proper embryonic patterning and cell fate during development [23]. Secreted HH ligands initiate signaling in receiving cells by binding and inactivating the transmembrane receptor PATCHED1 (PTCH1), which relieves its inhibition on the transmembrane protein SMOOTHENED (SMO). As a consequence, active SMO initiates an intracellular cascade that leads to the activation of the three GLI (zinc finger) transcription factors [24]. Transcriptional activation is mostly effected by GLI1 and GLI2, whereas GLI3 shows mainly repressor activity in the absence of ligands. In physiological conditions, Sonic Hh promotes the development of multipotent neural crest progenitors [25], from which melanocytes derive, and regulates proliferation of human melanocytes [26]. Similarly, it regulates brain stem cell lineages (e.g., 27–30) and skin stem cells (e.g., 31, 32). Aberrant activation of the HH-GLI signaling has been demonstrated in several types of human cancers [33]. The HH-GLI pathway is active and required for melanoma proliferation and xenograft growth in vivo [26] and GLI2 has been shown to drive melanoma invasion and metastasis [34]. HH-GLI signaling also regulates CSC survival and expansion in several types of cancer, such as glioma, colon, and gastric cancer, multiple myeloma, and myeloid leukemia [35–39].

In this study, we have isolated a population of human melanoma cells endowed with stem cell properties and high tumorigenic potential. We report that blockade of the HH-GLI pathway in melanoma stem cells, through chemical and genetic inhibition of SMO and GLI1, effectively reduces their self-renewal and tumor-initiation ability.

## MATERIALS AND METHODS

### Human Melanomas, Primary Cultures, and Melanospheres

A375 melanoma cells (CRL-1619) were obtained from ATCC (Manassas, VA, <http://www.lgcstandards-atcc.org>) and grown in Dulbecco's modified Eagle's medium (DMEM) (Euroclone, Milan, Italy, <http://www.euroclonegroup.it>) with 10% fetal bovine serum (FBS). Mycoplasma was periodically tested by 4',6-diamidino-2-phenylindole inspection and PCR. Melanoma samples were obtained from patients of the Plastic Surgery Unit of the S.M. Annunziata Hospital (Florence, Italy) and Dermatology Department and Medical-Surgical Critical Area of the University of Florence (Florence, Italy) after approved protocols by the

Ethics Committee. Tumors were incubated for 1 hour at 37°C with 1 mg/ml collagenase A and 20 µg/ml DNase I (Roche Applied Science, Basel, Switzerland, <http://www.roche-applied-science.com>) in DMEM/F12 (Euroclone). After dissociation and filtration, cells were grown in DMEM/F12 with 10% FBS and epidermal growth factor (EGF) (5 ng/ml) (Invitrogen, Carlsbad, CA, <http://www.invitrogen.com>) as already described [26]. Short-term cultures were obtained from 23 melanomas, of which two were from primary and 21 from metastatic melanomas (Table 1). SSM2c, M15c, and M26c cultures were cloned from the original metastases (SSM2, M15, and M26, respectively) by plating one cell per well. Patient-derived melanomas were passaged one to two times prior to RNA extraction and in vitro experiments. The expression of melanoma markers was verified on adherent cells by immunocytochemistry using anti-Melan A, anti-S100, and anti-Vimentin antibodies. For melanoma-sphere cultures, cells were seeded at a concentration of 5,000 cells per milliliter either in DMEM/F12 serum-free medium with N2 supplement, 20 µg/ml insulin, 10 ng/ml EGF, and 10 ng/ml basic fibroblast growth factor (bFGF) (Invitrogen) or in human embryonic stem cell medium (hESCM), as previously reported [14, 40].

### RNA Interference and Lentivectors

Lentiviruses were produced in HEK-293T cells as already described [41]. Lentiviral vectors pLKO.1-puro (LV-c), pLKO.1-puro-shSMO-64 (LV-shSMO-64) (targeting sequence 5'-GTGGA-GAAGATCAACCTGTTT-3'), pLKO.1-puro-shSMO-65 (LV-shSMO-65) (targeting sequence 5'-CCTGATGGACACAGAACTCAT-3'), pLKO.1-puro-shGLI1-85 (LV-shGLI1-85) (targeting sequence 5'-CCTGATTATCTTCCTCAGAA-3'), and pLKO.1-puro-shGLI1-87 (LV-shGLI1-87) (targeting sequence 5'-CCAAACGCTATACAGATCCTA-3') were from Open Biosystems (Lafayette, CO, <https://www.openbiosystems.com>). Most of the experiments have been performed using LV-shSMO-64 and LV-shGLI1-85.

### Self-Renewal Assay and Treatments

For self-renewal assay, melanospheres were dissociated and plated in 96-well plates at one cell per well or in 12-well plates at one cell per microliter dilutions. Cyclopamine (TRC, Toronto, Canada, <http://www.trc-canada.com>) (5 and 10 µM) [42] and tomatidine (10 µM) treatments were performed for 7 days, GANT61 treatment (Sigma, St. Louis, MO, <http://www.sigmaaldrich.com>) (0.5, 1, and 2.5 µM) [43] was carried out for 3 days in DMEM/F12 or hESCM medium containing 2 ng/ml EGF and bFGF. After treatment, spheres were dissociated, counted, and plated for self-renewal assay without the drugs. After 1 or 2 weeks, spheres were counted. All the experiments were performed in triplicate and were repeated at least three times.

### Aldefluor Assay and Flow Cytometry

The Aldefluor kit (Stem Cell Technologies, Vancouver, Canada, <http://www.stemcell.com>) was used to profile and separate cells with high and low ALDH activity (ALDH<sup>high</sup> and ALDH<sup>low</sup>), following manufacturer's protocol. Dissociated cells were incubated in Aldefluor assay buffer containing the ALDH protein substrate for 30 minutes at 37°C. Sorting gates for fluorescence-activated cell sorting (FACS) were drawn relative to cell baseline fluorescence, which was determined by the addition of the ALDH-specific inhibitor diethylaminobenzaldehyde (DEAB) during the incubation. DEAB-treated samples served as negative controls. Cells derived from xenografts were resuspended in Aldefluor buffer for the subsequent staining with the phycoerythrin-labeled monoclonal TRA-1-85 (BD Bioscience, San Diego, CA, <http://www.bdbiosciences.com>), which recognizes human cells and thus enables us to distinguish human from mouse cells. Nonviable cells were identified by propidium iodide staining. Flow cytometry was performed on a FACSCanto II (BD Bioscience). Cells were sorted by a FACS Aria (BD Bioscience) and the purity of sorted cells was assayed after the sorting was completed.

**Table 1.** Clinical features of melanomas used in this study and percentage of ALDH<sup>high</sup> cells

| Patient sample | Gender/age | Type | Site      | Location          | Breslow <sup>a</sup> | Stage | Sphere | %ALDH <sup>high</sup> cells | Follow up |
|----------------|------------|------|-----------|-------------------|----------------------|-------|--------|-----------------------------|-----------|
| SSM1           | M, 55      | MM   | Skin      | Trunk             | 8.5                  | IIIB  |        | 25.5                        | Deceased  |
| SSM2           | M, 55      | MM   | Skin      | Trunk             | 8.5                  | IIIB  | +      | 42                          |           |
| SSM2c          |            |      |           |                   |                      |       | +      | 51.9                        |           |
| M2             | M, 66      | MM   | LN        | Armpit            | 0.4                  | IIIC  | –      | 4.9                         | Alive     |
| M3L            | F, 84      | MM   | LN        | Groin             | 6.4                  | IIIC  | –      | 6.7                         | Alive     |
| M3R            |            |      | LN        | Groin             |                      | IIIC  | +      | 8.8                         |           |
| M5             | M, 65      | MM   | Skin      | Arm               | 1.1                  | IIIB  | +      | 9.8                         | Alive     |
| M6             | M, 79      | MM   | LN        | Arm               | N/A                  | IIIC  | –      | 3.4                         | Alive     |
| M8             | F, 59      | MM   | LN        | Groin             | 6.9                  | IV    | –      | 2.8                         | Alive     |
| M9             | F, 74      | MM   | Skin      | Arm               | N/A                  | IV    | –      | 1.8                         | Alive     |
| M11            | M, 76      | MM   | Skin      | Trunk             | 9.3                  | IIIC  | –      | 4                           | Alive     |
| M13            | M, 44      | MM   | Pancreas  | N/A               | N/A                  | IV    | –      | 2                           | Alive     |
| M14            | F, 79      | MM   | Skin      | Leg               | 8.1                  | IIIC  | +      | 20.5                        | Alive     |
| M15            | M, 85      | MM   | Skin      | Scalp             | 11                   | IIC   | N/A    | N/A                         | Deceased  |
| M15c           |            |      |           |                   |                      |       | +      | 46.8                        |           |
| M16            | M, 88      | PM   |           | Cheek             | 10                   | IIB   | +      | 19.8                        | Alive     |
| M17P           | M, 80      | PM   |           | Trunk             | i.s. regr            | IVb   | –      | 6                           | Alive     |
| M17M           | M, 80      | MM   | Skin      | Clavicular region | i.s. regr            | IVb   | –      | 2.2                         |           |
| M20            | N/A        | MM   | Skin      | Scalp             | 11                   | IVa   | –      | N/A                         | Alive     |
| M21            | M, 87      | MM   | Skin      | Trunk             | 5                    | IIIC  | +      | 44                          | Alive     |
| M22            | F, 80      | MM   | Skin      | Arm               | 2.6                  | IIIC  | –      | N/A                         | Deceased  |
| M25            |            |      | Skin      | Leg               |                      | IV    | –      | 2.6                         |           |
| M26            | F, 79      | MM   | LN        | Groin             | 0.47                 | IV    |        | 6.9                         | Alive     |
| M26c           |            |      |           |                   |                      |       | +      | 36.6                        |           |
| M27            | M, 71      | MM   | LN        | Groin             | 1.2                  | IV    | +      | 10.9                        | Alive     |
| M28            | M, 82      | MM   | LN        | Armpit            | 2.35                 | IIIC  | –      | 5                           | Alive     |
| A375           |            |      | Cell line |                   |                      |       | +      | 28                          |           |

<sup>a</sup>Thickness (mm) of the primary melanoma from which metastasis originated. i.s. regr: melanoma in situ with marker regression. N/A: data not available/not performed. SSM1 and SSM2 were two skin metastases that were excised from the same individual 1 and 4 months after diagnosis, respectively. M3L and M3R were two LN metastases excised from the same patient from a bilateral inguinal lymphadenectomy. M17P and M17M were a primary and metastatic melanomas, respectively, excised from the same individual. M22 and M25 were two skin metastases from the same patient, excised 1 and 5 months after diagnosis, respectively. SSM2c, M15c, and M26c were cloned from the original metastases (SSM2, M15, and M26, respectively).

Abbreviations: ALDH, aldehyde dehydrogenase; LN, lymph node; MM, metastatic melanoma; PM, primary melanoma.

## Immunocytochemistry and In Situ Hybridization

Formalin-fixed paraffin-embedded sections were subjected to immunocytochemical staining with mouse anti-human ALDH1 (clone 44/ALDH) (BD Biosciences, 611194) [44] and rabbit anti-human SMO (Abcam, Cambridge, U.K., Ab38686, <http://www.abcam.com>) antibodies. Briefly, after deparaffinization/hydration and antigen retrieval, performed with citrate buffer pH 6.0, slides were incubated with the primary antibody followed by incubation with a secondary antibody and visualization using AEC (Invitrogen) for ALDH1 or UltraVision Detection System (Lab Vision, Fremont, CA) and diaminobenzidine (DAB) (Dako, Carpinteria, CA, <http://www.dako.com/>) for SMO, according to manufacturer's recommendations. For GLI1 immunofluorescence, melanomaspheres were fixed with 4% formaldehyde, permeabilized with 0.1% Triton X-100 in phosphate buffered saline (PBS), blocked with 10% goat serum, and incubated with rabbit anti-GLI1 antibody (Abcam, Ab49314) and an anti-rabbit FITC secondary antibody. In situ hybridization with digoxigenin-labeled antisense RNA probe for *GLI1* was as previously described [26].

## Quantitative Real-Time PCR

Total RNA was isolated with TriPure Isolation Reagent (Roche Applied Science), subjected to DNase I treatment (Roche Applied Science), and checked for integrity. Reverse transcription was performed with High Capacity cDNA Reverse Transcription Kit (Applied Biosystems, Carlsbad, CA, <http://www.appliedbiosystems.com>). Quantitative real-time PCR (qRT-PCR) amplifications were carried out at 60°C using Power SYBR Green PCR Master Mix (Applied Biosystems) on a 7500 Fast Real-Time PCR System (Applied Biosystems) and analyzed by  $\delta\text{-}C_t$  method using

glyceraldehyde 3-phosphate dehydrogenase and  $\beta\text{-ACTIN}$  as housekeeping genes. Primer sequences are listed in supporting information Table S1.

## Western Blot

Western blot was carried out as previously described [41]. Antibodies used were rabbit polyclonal anti-GLI1 (Abcam, Ab49314), rabbit polyclonal anti-SMO (Abcam, Ab38686), mouse anti-ALDH1 (BD Biosciences), and anti-HSP90 (Heat Shock Protein 90) (Santa Cruz Biotechnology, Santa Cruz, CA, <http://scbt.com>). Chemiluminescent detection was used.

## Mouse Xenografts of Human Melanomas

In vivo experiments were conducted in accordance with National Guidelines and approved by Ethical Committee of Animal Welfare Office of Italian Health Ministry. Six- to eight-week-old female athymic nude mice (Foxn1 nu/nu) (Harlan Laboratories, Indianapolis, IN, <http://www.harlan.com>) were injected subcutaneously (s.c.) in lateral flanks with  $10^1$ ,  $10^2$ , and  $10^3$  cells from SSM2c spheres;  $10^3$  FACS-sorted ALDH<sup>high</sup> and ALDH<sup>low</sup> SSM2c cells;  $10^3$  FACS-sorted ALDH<sup>high</sup> SSM2c cells transduced with either pLKO.1-puro, pLKO.1-puro-shSMO, or pLKO.1-puro-shGLI1 lentiviruses. Cells were resuspended in Matrigel (BD Biosciences)/DMEM (1/1) before inoculation. Animals were monitored daily, subcutaneous tumor size was measured every 2–3 days by a caliper, and tumor volumes were calculated using the formula  $V = W^2 \times L \times 0.5$ , where  $W$  and  $L$  are tumor width and length, respectively.

## Statistical Analysis

Data are presented as means  $\pm$  SEM from at least three independent experiments. Statistical analysis of the data was



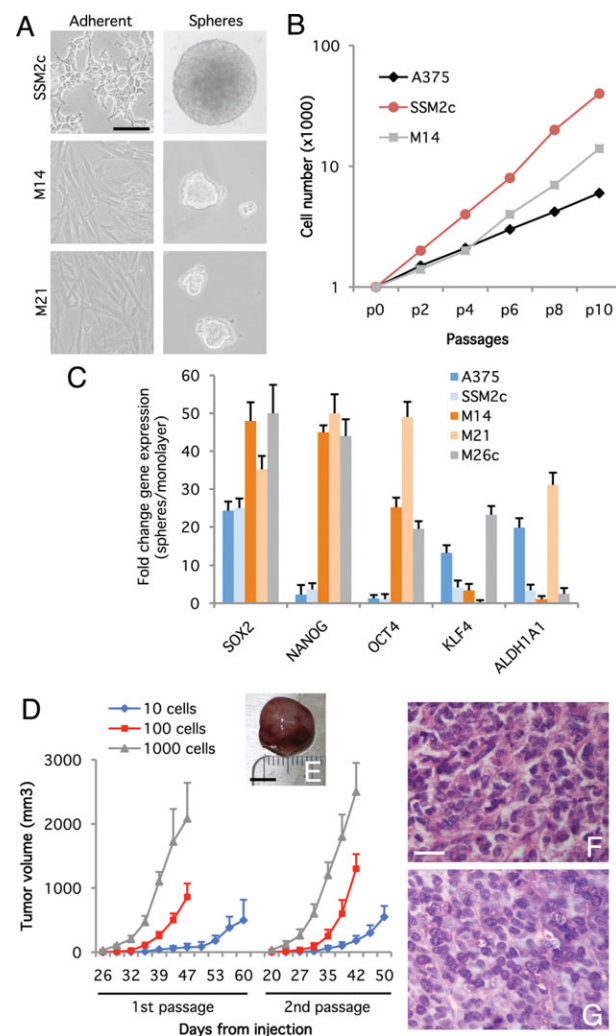


**Figure 1.** Human melanoma cells grown as spheres display stem cell-like features and tumorigenic ability. (A): Patient-derived adherent melanoma cells (SSM2c, M14, and M21) (left panels) form floating spheres (right panels) under serum-free conditions (scale bar = 100  $\mu$ m). (B): Growth of melanomasphere cultures. Total cell number is reported over 10 passages. (C): Quantitative real-time PCR (qRT-PCR) analysis of stem cell marker transcripts in patient-derived melanoma cells (SSM2c, M14, M21, and M26c) and A375 cell line. qRT-PCR values reflect  $C_t$  values after normalization with two housekeeping genes and are shown as fold change in spheres versus monolayer. (D): Tumorigenic potential of melanomaspheres. Growth curves of primary (first passage) and secondary (second passage) melanoma xenografts, generated by injection of different doses of melanomaspheres-derived SSM2c cells ( $n = 8$  for each group). (E): Representative pictures of a subcutaneous tumor (scale bar = 5 mm). (F, G): H&E staining of a melanoma from SSM2 patient (F) and from a melanoma xenograft in mouse derived from SSM2c spheres (G) (scale bar = 100  $\mu$ m). Abbreviation: ALDH1A1, aldehyde dehydrogenase 1 isoform A1.

performed by two-tailed Student's  $t$  test.  $p$  values of  $\leq .05$  were considered statistically significant.

## RESULTS

### Melanomaspheres Display Stem Cell-Like Features and Tumor-Initiation Ability

Growth of melanoma cells as spheres in human embryonic or neural stem cell media has been shown to support the selec-

tion of self-renewing cells enriched in CSC/TIC [14, 15, 45]. Two primary and 21 metastatic melanomas, of which 12 skin, eight lymph node, and one pancreas metastases, were used (Table 1). Melanomasphere cultures were established from metastatic melanomas SSM2c, M3R, M5, M14, M15c, M16, M21, M26c, and M27 and the melanoma cells A375 (Table 1 and Fig. 1A). Self-renewal ability of melanomaspheres was assessed by dissociating primary spheres to single cell and growing them at clonal density of one cell per microliter or at limiting dilution (one cell per well). Single melanomasphere cells generated secondary clones that could be redissociated and regenerate new spheres from single cells for at least 10 passages (Fig. 1B). All short-term cultures expressed S100 or Melan-A (supporting information Fig. S1) and the melanocyte-specific microphthalmia-associated transcription factor (*MITF-M*) mRNA (supporting information Fig. S2), demonstrating their melanogenic origin. qRT-PCR analysis showed that expression levels of embryonic stem cell pluripotency factors *SOX2*, *NANOG*, *OCT4*, and *KLF4* and the stem cell marker ALDH1 isoform A1 were high in melanomaspheres (Fig. 1C).

Tumorigenicity of melanomaspheres was assessed by evaluating their capacity to form tumors when s.c. injected into athymic nude mice. At a dose of  $10^3$  cells, 100% of the injection sides generated primary tumors (Fig. 1D and supporting information Fig. S3). Notably, SSM2c cells could form tumors when as few as 10 cells were injected (Fig. 1D, 1E). Melanomaspheres could be rederived from the xenotransplanted tumors and they could form secondary tumors, which developed in 100% of the injected mice and grew faster than their corresponding first passage (Fig. 1D). Human melanoma xenografts generated from melanomaspheres in nude mice closely resembled the histological features of the primary tumor from which they were derived (Fig. 1F, 1G). Altogether, these results indicate that cells from melanomaspheres have self-renewal ability, express high levels of embryonic stem cell pluripotency factors, and are able to sustain tumor growth in vivo, suggesting that melanomaspheres possess the fundamental properties of CSC.

### Human Melanomas Contain a Population with High ALDH Activity

It has been shown that cells with high ALDH activity (ALDH<sup>high</sup>) are enriched in CSC in a variety of tumor types [44, 46–48], including melanoma [20]. We used the Aldefluor assay to quantify the percentage of ALDH<sup>high</sup> cells in two primary melanomas and 19 melanoma metastases, of which 10 from skin, eight from lymph nodes, and one from pancreas. A percentage of ALDH<sup>high</sup> cells, ranging from 1.8% to 51.9% of the total viable cells, was detected by flow cytometry in all the melanomas tested (Table 1 and Fig. 2A). Interestingly, skin metastases showed the highest percentage of ALDH<sup>high</sup> cells (>10%), compared to lymph node and pancreas metastases (Fig. 2B). Our analysis shows that only tumors with a percentage of ALDH<sup>high</sup> cells near to 10% or higher formed spheres in culture (Table 1), suggesting a good correlation between ALDH<sup>high</sup> activity and spheres formation efficiency. qRT-PCR analysis showed a positive correlation between the percentage of ALDH<sup>high</sup> cells and *NANOG* expression ( $R^2 = 0.71$ ) (Fig. 2C), suggesting an abundance of CSC in this population.

To examine the relationship between ALDH expression and clinical malignant melanoma progression and to assess its potential use as a marker for melanoma stem cells, we analyzed ALDH1 expression by immunocytochemistry in four major diagnostic types: 10 normal and 10 dysplastic/atypical melanocytic nevi, 10 thin (<1 mm) and 10 thick (>1 mm) primary melanomas, and 10 metastatic melanomas. We found

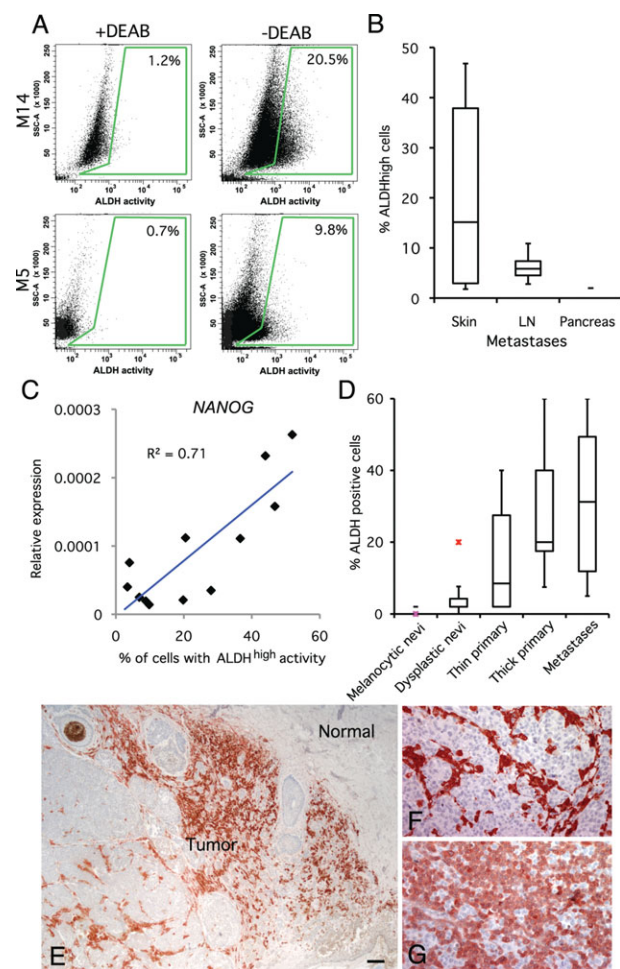


**Figure 2.** Human melanomas contain cells with high ALDH activity. (A): Flow cytometry analysis of two representative patient-derived metastatic melanomas (M14 and M5) using the Aldefluor assay. Baseline fluorescence was established by inhibiting ALDH activity with DEAB (left) and used to generate a gate that will identify ALDH<sup>high</sup> cells in melanoma cells incubated without DEAB (right). (B): Percentage of ALDH<sup>high</sup> cells in skin ( $n = 10$ ), lymph node ( $n = 8$ ), and pancreas ( $n = 1$ ) metastases, determined by flow cytometry. (C): Linear correlation analysis between *NANOG* expression, measured by quantitative real-time PCR, and ALDH activity, measured by flow cytometry, shows a positive correlation between *NANOG* expression and the percentage of ALDH<sup>high</sup> cells. (D): Quantification of the percentage of ALDH1-positive cells in melanocytic nevi ( $n = 10$ ), dysplastic nevi ( $n = 10$ ), thin ( $n = 10$ ) and thick ( $n = 10$ ) primary melanomas, and melanoma metastases ( $n = 10$ ), as determined by immunocytochemistry. Red crosses indicate outlier values. (E-G): ALDH1 immunocytochemistry in a primary melanoma (E), a lymph node (F), and a skin metastasis (G). Note the localization of ALDH-positive cells in the tumor-normal tissue interface (E). Scale bar = 200  $\mu\text{m}$  (E) and 60  $\mu\text{m}$  (F, G). Abbreviations: ALDH, aldehyde dehydrogenase; DEAB, diethylaminobenzaldehyde; LN, lymph node.

that primary and metastatic melanomas contained more cells expressing ALDH1 than normal and dysplastic melanocytic nevi. Nevi showed only few positive cells (Fig. 2D and supporting information Table S2) and weak dermal staining in the microvasculature, hair follicles, and sebaceous glands (data not shown), as previously reported [49]. We also detected more ALDH1-positive cells in thick primary melanomas and melanoma metastases than in thin primary melanomas (Fig. 2D and supporting information Table S2). Notably, in most of the primary melanomas, ALDH1 was highly

expressed in tumor cells at the tumor-host interface (Fig. 2E), suggesting that the ALDH1-positive cells might be mainly localized at the invading tumor front. ALDH1 was expressed in all thick primary and metastatic melanomas, with ALDH<sup>high</sup> cells representing approximately 5% to 50%–60% of tumor cells (Fig. 2F, 2G, supporting information Table S2), consistent with cytometric Aldefluor analysis.

### Enhanced Self-Renewal and Tumorigenicity of ALDH<sup>High</sup> Melanoma Cells

To determine whether the subset defined by high ALDH activity (ALDH<sup>high</sup>) was enriched in CSC/TIC, we compared the ability of FACS-sorted ALDH<sup>high</sup> versus ALDH<sup>low</sup> melanoma cells to self-renew in vitro and to initiate tumor formation in vivo, using SSM2c and A375 cells. Self-renewal assay showed that ALDH<sup>high</sup> cells produced more spheres than the ALDH<sup>low</sup> population (Fig. 3A, 3B). Gene expression analysis revealed that ALDH<sup>high</sup> population expressed higher level of stem cell markers *SOX2*, *OCT4*, and *NANOG* than the ALDH<sup>low</sup> population (Fig. 3C). These data indicate that ALDH<sup>high</sup> melanoma cells display a stemness signature and have higher self-renewal ability than ALDH<sup>low</sup> melanoma cells. We next investigated the activation of the HH pathway in both subpopulations. GLI1 is one of the final effectors of the HH pathway and the best read out of an active pathway [50]. Recent reports suggest that in several types of cancer, including melanomas, GLI1 can be modulated by proliferative and oncogenic inputs, in addition to or independent of upstream HH signaling [24, 26, 51–54]. Therefore, we compared the expression of GLI1 protein in ALDH<sup>high</sup> and ALDH<sup>low</sup> cells. Western blot analysis revealed that ALDH<sup>high</sup> cells expressed higher level of GLI1 as compared to the ALDH<sup>low</sup> population (Fig. 3D).

To test the tumorigenicity of the ALDH<sup>high</sup> subpopulation,  $10^3$  isolated ALDH<sup>high</sup> and ALDH<sup>low</sup> cells from SSM2c and A375 spheres were injected s.c. into athymic nude mice. The tumors generated from ALDH<sup>high</sup> of both SSM2c (Fig. 3E, 3F) and A375 cells (supporting information Fig. S4) were significantly larger and grew faster than tumors originated from ALDH<sup>low</sup> cells. Western blot analysis of SSM2c xenografts, dissected 38 days after the injection, showed higher expression of GLI1 protein in tumors derived from ALDH<sup>high</sup> cells than in those from ALDH<sup>low</sup> cells (Fig. 3G), suggesting that ALDH<sup>high</sup> cells maintain high HH pathway activity in vivo. Consistently, in situ hybridization analysis confirmed that tumors derived from ALDH<sup>high</sup> cells presented higher level of *GLI1* mRNA than those derived from ALDH<sup>low</sup> cells (supporting information Fig. S5).

We next compared the ability of ALDH<sup>high</sup> and ALDH<sup>low</sup> cells to re-establish tumor heterogeneity. Primary tumors were harvested and reanalyzed both by the Aldefluor assay to elucidate their ALDH phenotype after in vivo growth and by anti-human TRA-1 antibody to distinguish human cells. Reanalysis of tumors produced from sorted ALDH<sup>high</sup> tumor cells revealed a mixed population that contained 6.5% of ALDH<sup>high</sup>/hTRA<sup>+</sup> cells. In contrast, ALDH<sup>low</sup> tumors were found to possess only a very small residual ALDH<sup>high</sup>/hTRA<sup>+</sup> cell subpopulation (Fig. 3H). This result confirms higher abilities of the ALDH<sup>high</sup> cells to re-establish tumor heterogeneity in vivo, consistently with the existence of a cellular hierarchy in melanomas with respect to ALDH.

### Inhibition of HH-GLI Signaling Decreases Self-Renewal of Melanoma Stem Cells

The ALDH<sup>high</sup> phenotype is associated with high HH activity, enhanced self-renewal and tumorigenicity, consistent with the idea that ALDH<sup>high</sup> population is enriched in melanoma stem

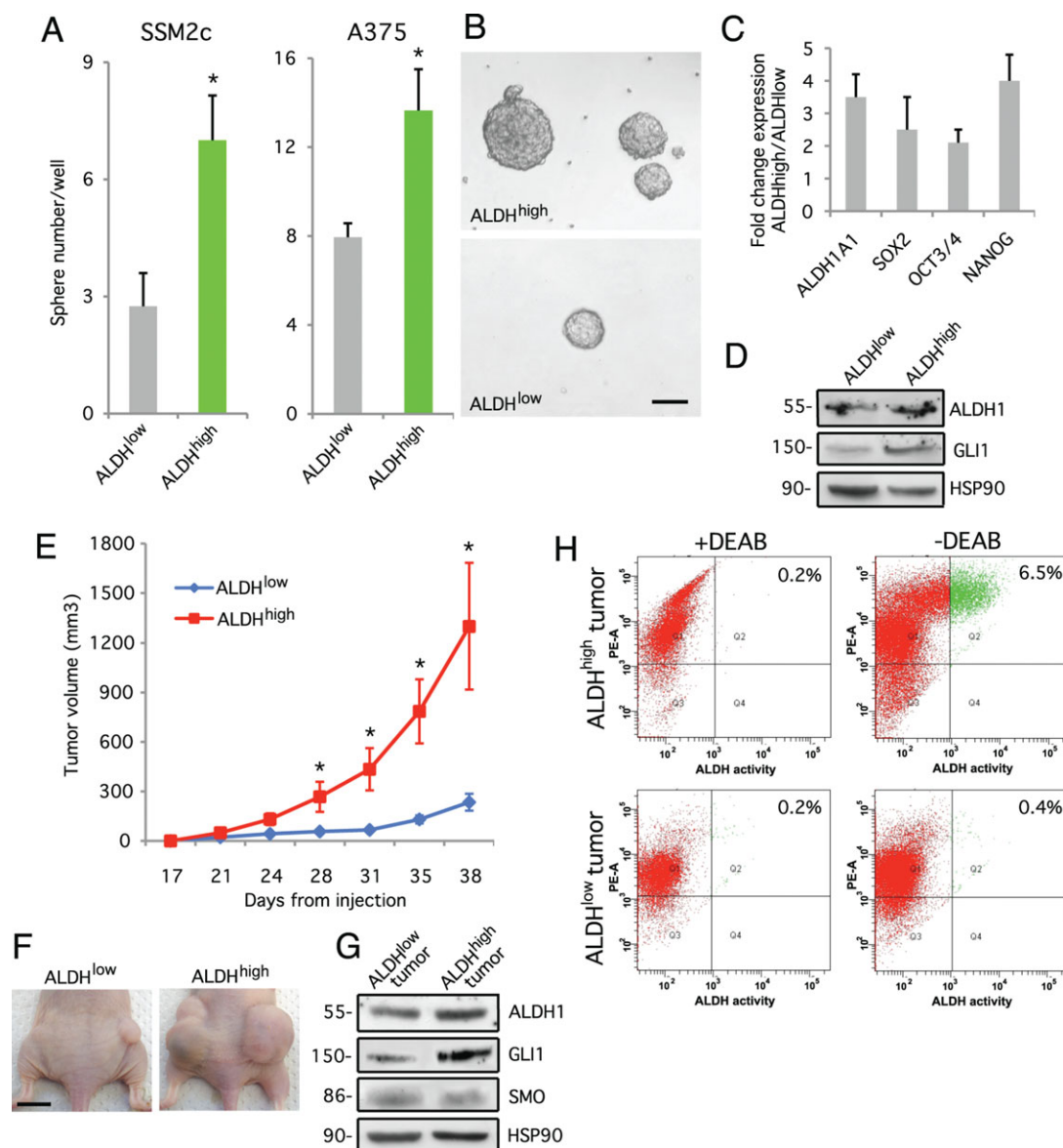


**Figure 3.** ALDH<sup>high</sup> human melanoma cells exhibit enhanced self-renewal and tumorigenicity and harbor active Hedgehog pathway. (A): Sphere formation efficiency of fluorescence-activated cell sorting (FACS)-sorted ALDH<sup>high</sup> and ALDH<sup>low</sup> SSM2c and A375 cells \*,  $p < .05$ . (B): Representative pictures of ALDH<sup>high</sup> and ALDH<sup>low</sup> SSM2c spheres (scale bar = 50 μm). (C): Gene expression analysis of ALDH<sup>high</sup> SSM2c cells, as measured by quantitative real-time PCR.  $C_t$  values were normalized with the average of the values of two housekeeping genes and shown as ALDH<sup>high</sup>/ALDH<sup>low</sup> ratios. (D): Western blot of FACS-sorted ALDH<sup>low</sup> and ALDH<sup>high</sup> SSM2c cells showing the expression level of ALDH1 and GLI1 proteins. HSP90 was used as control. (E): Tumor growth curves were generated from  $10^3$  FACS-sorted ALDH<sup>high</sup> and ALDH<sup>low</sup> SSM2c cells ( $n = 12$  for each group) \*,  $p < .05$ . (F): Representative images of (E) (scale bar = 10 mm). (G): Western blot of tumors derived from ALDH<sup>low</sup> and ALDH<sup>high</sup> cells showing endogenous levels of ALDH1, GLI1, and SMO proteins. HSP90 is used as control. (H): ALDH activity was assayed in tumors derived from ALDH<sup>high</sup> and ALDH<sup>low</sup> cells, with DEAB-treated cells used as a negative control. Cells were at the same time analyzed with anti-human TRA-1 antibody, to allow the discrimination from mouse cells. It shows that ALDH<sup>high</sup> tumors possess a greater proportion of ALDH<sup>high</sup> cells (6.5%) than ALDH<sup>low</sup> tumors (0.4%). Abbreviations: ALDH, aldehyde dehydrogenase; DEAB, diethylaminobenzaldehyde; GLI1, GLI family zinc finger 1; SMO, SMOOTHENED.

cells. To test whether HH-GLI function is involved in maintenance of the ALDH<sup>high</sup> melanoma cells, we inhibited the HH pathway by knocking down SMO. Silencing of SMO was achieved by two independent shRNAs expressed from replication of incompetent puromycin-resistant lentivectors: shSMO-64 and shSMO-65 (supporting information Fig. S6). FACS analysis revealed a drastic decrease in the fraction of ALDH<sup>high</sup> cells (from 52.6% to 2.5%) in SSM2c cells transduced with shSMO (Fig. 4A). Western blot analysis showed that silencing of SMO in SSM2c cells led to a loss of endogenous

SMO and GLI1 proteins (Fig. 4B), confirming the efficient inhibition of these HH components. To further assess the role of the transcription factor GLI1 itself in maintaining the ALDH<sup>high</sup> melanoma stem cells, we silenced specifically GLI1, using two independent shRNA: shGLI1-85 and shGLI1-87 (supporting information Fig. S7). FACS analysis revealed a smaller population of ALDH<sup>high</sup> cells in SSM2c transduced with shGLI1 (from 52.6% to 15.4%) (Fig. 4A), consistent with the results obtained by inhibiting SMO. GLI1 silencing resulted in an efficient inhibition of endogenous



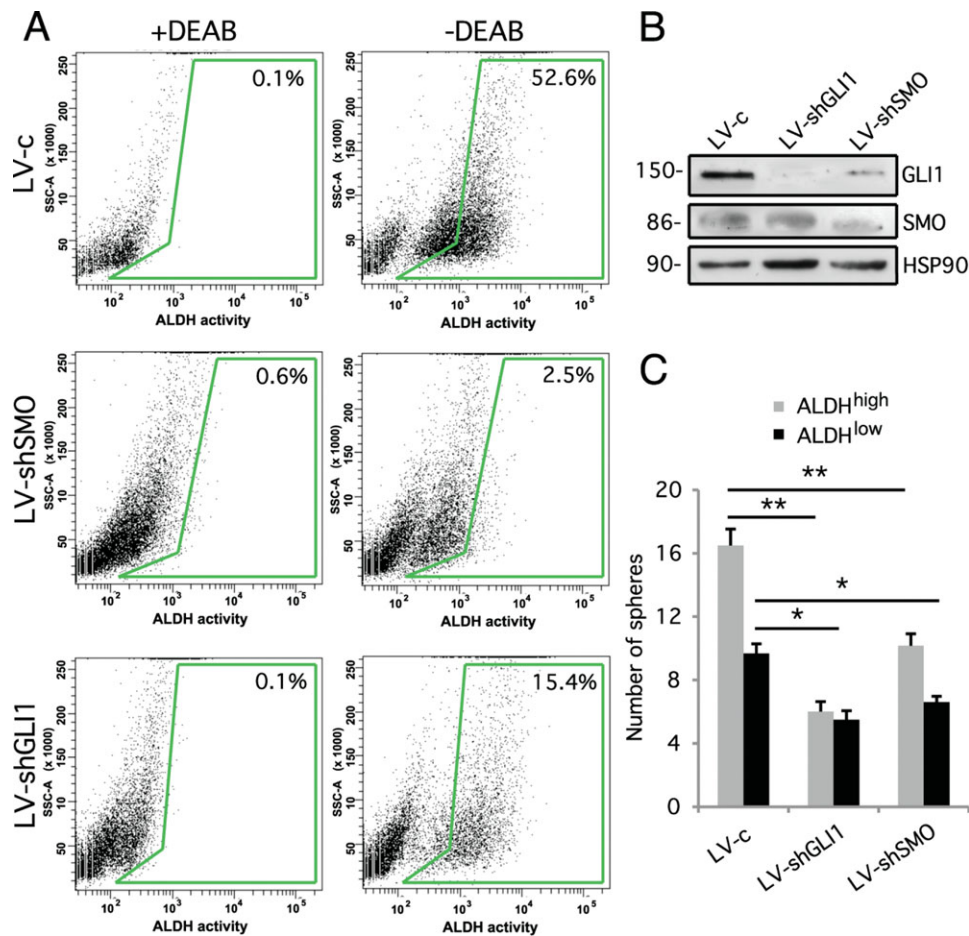


**Figure 4.** Requirement of Hedgehog-Gli function in ALDH<sup>high</sup> melanoma stem cells. (A): Aldefluor assay of SSM2c cells expressing LV-c, LV-shSMO, or LV-shGLI1, showing a drastic reduction of ALDH<sup>high</sup> cells after silencing of SMO (LV-shSMO) and GLI1 (LV-shGLI1). (B): Western blot of SSM2c cells transduced with LV-c control, LV-shGLI1, and LV-shSMO, showing a near loss of GLI1 expression in LV-shGLI1 and LV-shSMO and a reduced SMO expression in LV-shSMO. HSP90 was used as loading control. (C): Number of secondary spheres in ALDH<sup>high</sup> and ALDH<sup>low</sup> SSM2c cells after silencing of GLI1 (LV-shGLI1) and SMO (LV-shSMO) (\*,  $p < .05$ ; \*\*,  $p < .001$ ). Abbreviations: ALDH, aldehyde dehydrogenase; DEAB, diethylaminobenzaldehyde; GLI1, Gli family zinc finger 1; LV, lentiviral vector; SMO, SMOOTHENED.

GLI1, as indicated by the complete loss of GLI1 protein in SSM2c cells (Fig. 4B). We next assessed the effect of HH pathway inhibition on self-renewal ability. Silencing of SMO and GLI1 reduced self-renewal of ALDH<sup>high</sup> melanoma cells ( $p \leq .001$ ) and, at lesser extent, that of ALDH<sup>low</sup> melanoma cells ( $p \leq .05$ ) (Fig. 4C). This result correlates with the higher expression of GLI1 in ALDH<sup>high</sup> population (Fig. 3D). Altogether, these findings indicate that ALDH<sup>high</sup> cells are more sensitive to SMO and GLI1 inhibition than ALDH<sup>low</sup> cells, suggesting a dependence on HH-Gli activity for survival and self-renewal.

As an alternative approach to test the involvement of the HH pathway in melanoma stem cells, we have used melanomasphere cultures, which self-renew and mimic the original tumor after transplantation into athymic nude mice (Fig. 1F, 1G). GLI1 is highly expressed in melanomaspheres with a prevalent nuclear localization, as shown by immunofluorescence (Fig. 5A). qRT-PCR analysis showed that also *SHH*, *PTCH1*, *SMO*, *GLI2*, *GLI3* and the targets *HIP1* and vascular endothelial growth factor A were highly expressed in melanomaspheres (supporting information Fig. S8). To test for a role of HH-Gli signaling in regulating melanomasphere self-renewal, we knocked down SMO and GLI1. Silencing of SMO diminished the number of A375 and SSM2c spheres by 75% and 70%, respectively (Fig. 5B, 5D). Self-renewal assay

showed that GLI1 silencing reduced the number of A375 and SSM2c secondary clones by 48% and 64%, respectively (Fig. 5C, 5D). Western blot analysis showed that silencing of SMO and GLI1 in melanomaspheres completely knocked down GLI1 protein (Fig. 5E, upper panel) and *GLI1* and *SMO* mRNA levels (Fig. 5E, lower panel). As an additional test to investigate the requirement of HH-Gli function, we also inhibited SMO pharmacologically by treatment with cyclopamine, a plant alkaloid [55] that inhibits SMO [42, 56, 57] and that we found it to be a specific inhibitor of HH-Gli (e.g., 26, 35, 36, 58). Melanomaspheres were treated for 7 days with cyclopamine [35]. After the treatment, spheres were dissociated and we quantified the ability of single cells to generate secondary spheres in absence of the drug. Consistently with silencing of SMO, cyclopamine treatment led to a significant and dose-dependent reduction of the ability to form secondary spheres (Fig. 5F). Similarly, chemical inhibition of GLI1 and GLI2 with GANT61 [43, 59, 60] resulted in a dose-dependent decrease in spheres number (Fig. 5G). Altogether, these results indicate that SMO and GLI1 are critical to maintain self-renewal of melanoma stem cells.

To complement these studies, we investigated whether activation of the HH pathway in adherent cells could enhance the number of putative melanoma stem cells. FACS analysis showed that activation of the HH pathway by silencing of *PTCH1* [41],



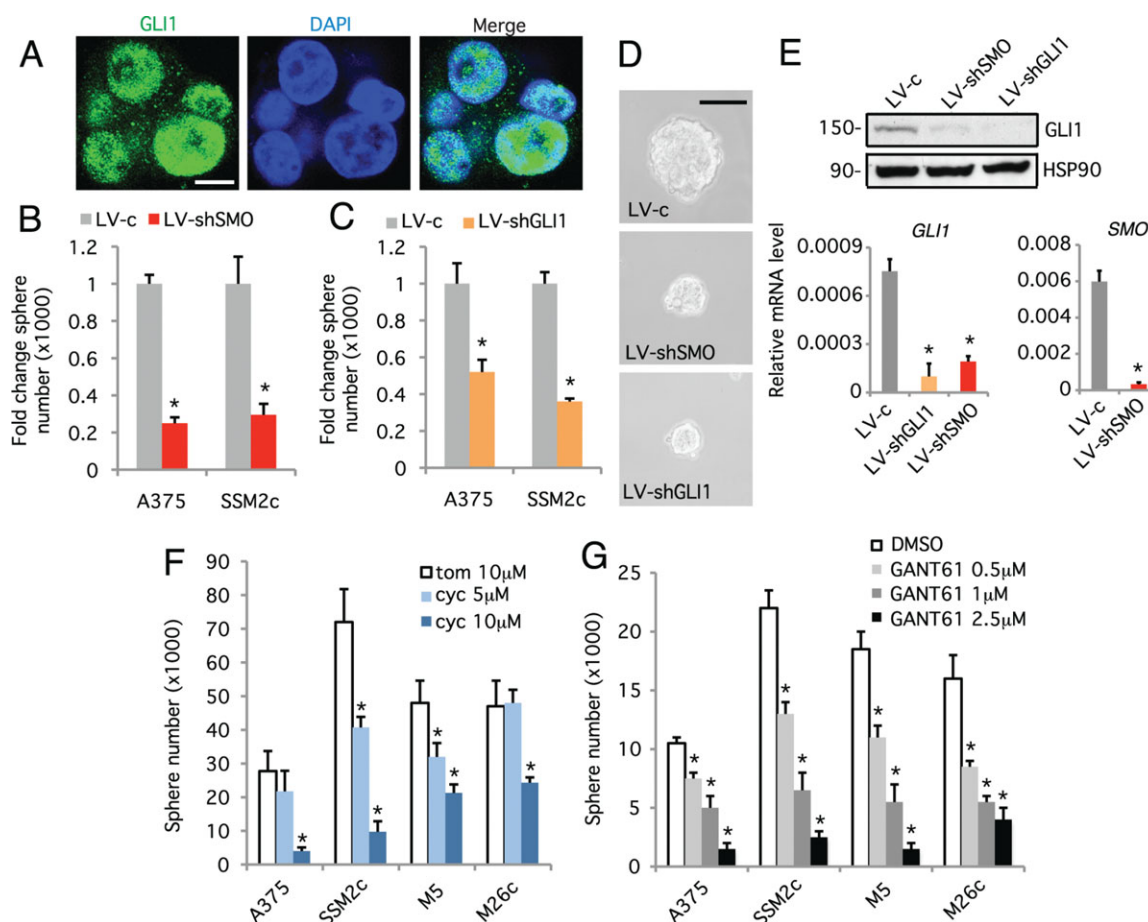


**Figure 5.** Genetic and chemical inhibition of HH-GLI pathway reduces self-renewal of melanomaspheres. (A): Confocal images of SSM2c melanomaspheres after immunolabeling with GLI1 antibody. Nuclei were counterstained with DAPI (scale bar = 10  $\mu$ m). (B, C): Reduction in the number of secondary melanomaspheres after silencing of SMO (LV-shSMO) and GLI1 (LV-shGLI1) in A375 and SSM2c cells. (D): Representative images of melanomaspheres as indicated in (B) and (C) (scale bar = 150  $\mu$ m). (E): Western blot (upper panel) and qRT-PCR (lower panels) analyses of SSM2c spheres transduced with LV-c control, LV-shSMO, and LV-shGLI1, showing the near complete loss of endogenous GLI1 protein (upper panel) and dramatic reduction of *GLI1* and *SMO* mRNA (lower panels). (F, G): Reduction in the number of secondary spheres in melanomaspheres treated for 7 days with SMO inhibitor cyclopamine (F) or for 3 days with GANT61 (G), a small-molecule inhibitor of both GLI1 and GLI2 \*,  $p < .05$ . Abbreviations: DAPI, 4',6-diamidino-2-phenylindole; DMSO, dimethyl sulfoxide; GLI1, GLI family zinc finger 1; GLI2, GLI family zinc finger 2; LV, lentiviral vector; SMO, SMOOTHENED.

an endogenous inhibitor of SMO, increased the number of A375 ALDH<sup>high</sup> melanoma cells (from 28.5% to 68.9%) and enhanced their self-renewal (supporting information Fig. S9).

### Inhibition of the HH-GLI Pathway Reduces Tumor-Initiation Ability of ALDH<sup>High</sup> Melanoma Cells

To test the role of the HH signaling in ALDH<sup>high</sup> melanoma stem cells in vivo, we engrafted s.c. into athymic nude mice  $10^3$  ALDH<sup>high</sup> SSM2c cells transduced with LV-shSMO, LV-shGLI1, and the control LV-c. Cell transduced with the control yielded rapidly growing tumors (Fig. 6A). Silencing of SMO and GLI1 greatly reduced tumor growth (Fig. 6A, 6B). Immunocytochemistry and in situ hybridization analyses of sections obtained from tumors dissected 30 days after injection showed a dramatic reduction of SMO protein expression in LV-shSMO tumors (Fig. 6C) and a decrease in *GLI1* mRNA expression in LV-shGLI1 tumors (Fig. 6C) compared to control sections (LV-c). These results indicate that the reduction of tumor growth depends on the specific silencing of SMO and GLI1. Consistently, Western blot analysis confirmed the downregulation of

SMO and GLI1 in LV-shSMO and LV-shGLI1 xenografts compared to the control tumors (LV-c) (Fig. 6D). These data suggest that an active HH signaling is required for growth in vivo of ALDH<sup>high</sup> melanoma stem cells.

## DISCUSSION

In this study, we show that human melanomas contain cells that resemble the properties of CSC, including the ability to self-renew, to express high levels of stem cell factors, and to be tumorigenic in immunocompromised mice. Interestingly, we find that the HH-GLI pathway is required to maintain self-renewal and tumor-initiating ability of these putative melanoma stem cells.

Our data show that melanomaspheres can be grown with high efficiency from bulk melanoma cells, and that these cells display in vitro self-renewal ability and sustain tumor growth in vivo by serial transplantation assay. Moreover, melanomaspheres can generate in vivo melanoma xenografts that recapitulate the phenotypic composition of the parental tumor from which the cells have been derived. These hallmarks

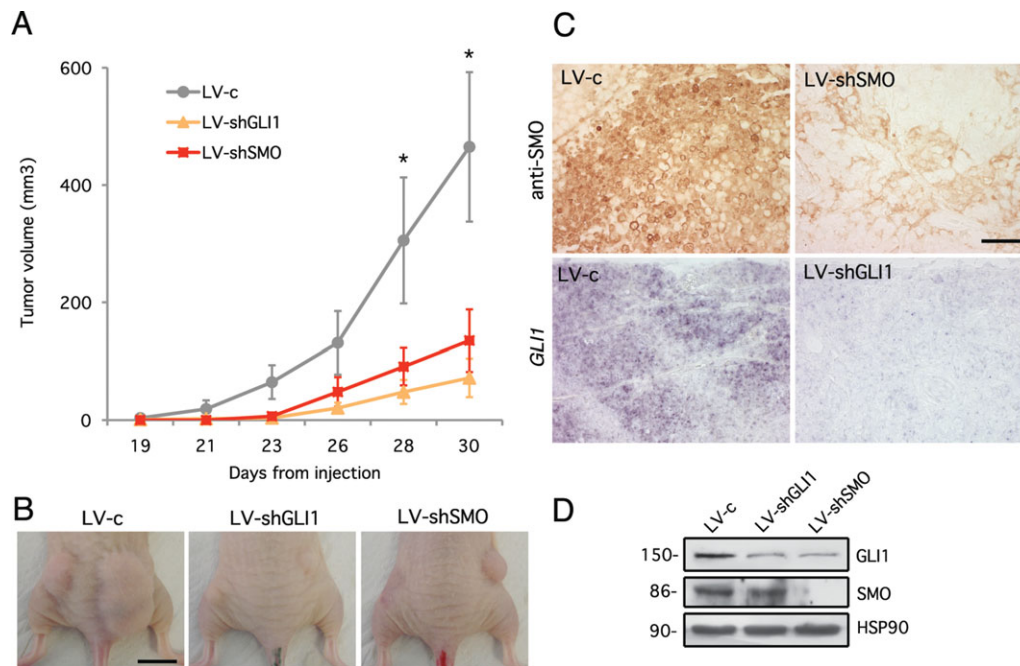


**Figure 6.** Inhibition of the HH-GLI signaling impairs in vivo growth of ALDH<sup>high</sup> melanoma stem cells. (A): Subcutaneous xenograft growth curves of FACS-sorted ALDH<sup>high</sup> SSM2c cells transduced with a LV-c control, LV-shGLI1, and LV-shSMO. For each group, 12 tumors were analyzed \*,  $p < .05$ . (B): Representative images of subcutaneous xenografts in nude mice taken at the same time for each group (scale bar = 10 mm). (C, D): Tumors from the mice in (A) and (B) were analyzed by immunocytochemistry for SMO (C, upper panels), by in situ hybridization for *GLI1* (C, lower panels) and Western blot for GLI1 and SMO proteins (D) (scale bar = 100  $\mu$ m). HSP90 was used as loading control. Abbreviations: GLI1, GLI family zinc finger 1; LV, lentiviral vector; SMO, SMOOTHENED.

resemble the properties of CSC [14, 15, 45], suggesting that melanomaspheres represent a good model to investigate melanoma stem cell biology. According to our gene expression analysis, melanomaspheres consistently express high levels of embryonic stem cell pluripotency factors *SOX2*, *NANOG*, *OCT4*, and *KLF4*, the cohort of genes that have been shown to reprogram normal differentiated cells to pluripotent embryonic stem cells [61]. This finding is confirmed by other studies [45, 62] and suggests a high differentiation potential of melanoma stem cells.

The aggressiveness of melanoma is due to the presence of highly tumorigenic populations that confer resistance to conventional therapy and embryonic-like differentiation ability [63, 64]. Therefore, novel therapeutic strategies that selectively target the most resistant and long-living cells within the tumor, the melanoma CSC/TIC, are needed. We have previously shown that human melanomas require HH pathway for proliferation and survival [26]. Here, we demonstrate for the first time that the HH-GLI signaling is critical for self-renewal in vitro and tumor initiation of melanoma stem cells. Functionally, the cell-autonomous modulation of HH-GLI signaling at the level of the transmembrane protein SMO and of the transcription factor GLI1 in vitro and in vivo by RNA interference defines melanoma stem cells as primary targets of HH-GLI signaling. Our data support the inhibition of HH-GLI as a promising novel therapeutic strategy for human melanoma.

Currently, no definitive consensus has been reached on CSC/TIC phenotype for melanoma, although several studies clearly support the existence within melanomas either of TIC endowed with stem cells features [13–20] or slow-cycling cells sustaining tumor growth [65, 66]. Our functional data on sorted ALDH<sup>high</sup> and ALDH<sup>low</sup> melanoma cells showed that ALDH<sup>high</sup> cells are more tumorigenic and clonogenic than

ALDH<sup>low</sup> cells. In addition, isolated ALDH<sup>high</sup> cells are able to recapitulate tumor heterogeneity for ALDH<sup>high</sup> and ALDH<sup>low</sup> cells in vitro and in vivo, whereas this ability was much less in isolated ALDH<sup>low</sup> cells, consistently with the existence of a cellular hierarchy in melanoma with respect to ALDH. ALDH<sup>high</sup> melanoma cells form fast growing tumors in athymic nude mice, whereas ALDH<sup>low</sup> cells are capable of forming very small, slow growing tumors. Further studies are needed to determine whether this indicates residual CSC activity in ALDH<sup>low</sup> cells or contamination with some ALDH<sup>high</sup> cells. Nevertheless, our data confirm the usefulness of ALDH activity to enrich for melanoma stem cells. Our findings are consistent with a previous report showing that ALDH selects tumorigenic melanoma cells in nonobese diabetic/severe combined immunodeficient (NOD/SCID) mice [20]. However, the use of a fully immunocompromised NOD/SCID/IL2 $\gamma$ <sup>null</sup> (NSG) mouse model suggested that ALDH activity does not select for cells with enhanced aggressive properties [40]. Because the main difference between NSG and nude or NOD/SCID mice is the absence of natural killer cells in NSG mice, the discrepancy between our data and this study [40] is likely due to the different level of immunocompetence of the xenotransplant recipients. The latter provides a permissive environment for tumor growth [19], and therefore it is less representative of the human immune status.

In this study, we show that human melanomas contain a fraction of cells with high ALDH activity, which varies from 2% to 52%. Skin metastases showed the highest percentage of ALDH<sup>high</sup> cells (Fig. 2B), as determined by flow cytometry. According to our immunocytochemical analysis, we detected more ALDH1-positive cells in metastases (most of which are from the skin) and thick primary melanomas than in thin melanomas. Interestingly, in most of the thick melanomas, ALDH1 was highly expressed in tumor cells at the tumor-host

interface (Fig. 2E), suggesting that the ALDH1-positive melanoma stem cells might be mainly localized at the invading tumor front. ALDH1-positive cells might therefore be involved in the formation of metastatic melanoma, whereas less aggressive tumors might originate from other types of melanoma-initiating cells. Notably, the aggressive biological behavior demonstrated in mice by isolated ALDH<sup>high</sup> cells and the high percentages of these cells detected in some rapidly lethal melanomas of our series (e.g., patients SSM2c and M15, which both died 1.5 year after diagnosis) induce to speculate that ALDH1 represents a melanoma stem cell marker that might correlate with a poor prognosis.

Here, we show for the first time that blockade of the HH-GLI pathway by interference with SMO or GLI1 decreases self-renewal and tumorigenicity of ALDH<sup>high</sup> melanoma stem cells. This finding confirms the results obtained with melanoma-sphere-derived CSC and suggest that HH-GLI is critical to maintain ALDH<sup>high</sup> melanoma stem cells. At present, it is unclear whether high ALDH activity is functionally involved in stem cells (normal or CSC) or it is only a useful marker to identify CSC/TIC. Because ALDH enzyme activity is frequently required for the detoxification of intracellular exogenous and endogenous aldehydes, it might protect skin (stem) cells from xenobiotics and in the meanwhile make them insensitive to chemotherapeutic agents (e.g., 67).

## CONCLUSIONS

Our data support the existence within human melanomas of a subpopulation made up of highly tumorigenic cells with features similar to embryonic stem cells, including extensive

self-renewal and a stemness signature. Whereas several forms of treatment can give temporary benefits, radical therapy for melanoma will rely on the ability to eliminate these subpopulations, irrespective of their number. Our study highlights the role of the HH signaling pathway in driving self-renewal and tumorigenicity of melanoma stem cells and points to SMO and GLI1 as novel and effective therapeutic targets for the treatment of human melanoma.

## ACKNOWLEDGMENTS

We thank Prof. Lucio Luzzatto and Dr. Laura Poliseno (Istituto Toscano Tumori) for helpful comments on the article and discussion. We are grateful to Dr. Carmelo Urso (S. Maria Annunziata Hospital, Florence, Italy) for help in obtaining samples, Dr. Massimo D'Amico, Dr. Elisabetta Rovida, and Eugenio Torre (Department of Pathology and Experimental Oncology, University of Florence, Italy) for assistance with flow cytometry, confocal microscopy, and histology. This work was supported by grants from Associazione Italiana per la Ricerca sul Cancro (AIRC, 9566), Regional Health Research Program 2009, and Fondazione Cassa di Risparmio di Firenze to B.S. S.P. was supported by AIRC fellowship.

## DISCLOSURE OF POTENTIAL CONFLICTS OF INTEREST

The authors indicate no potential conflicts of interest.

## REFERENCES

- Balch CM, Gershenwald JE, Soong SJ et al. Final version of 2009 AJCC melanoma staging and classification. *J Clin Oncol* 2009;27: 6199–6206.
- Kirkwood JM, Manola J, Ibrahim J et al. A pooled analysis of eastern cooperative oncology group and intergroup trials of adjuvant high-dose interferon for melanoma. *Clin Cancer Res* 2004;10: 1670–1677.
- Ko JM, Fisher DE. A new era: Melanoma genetics and therapeutics. *J Pathol* 2011;223:241–250.
- Flaherty KT, Puzanov I, Kim KB et al. Inhibition of mutated, activated BRAF in metastatic melanoma. *N Engl J Med* 2010;363: 809–819.
- Hodi FS, O'Day SJ, McDermott DF et al. Improved survival with ipilimumab in patients with metastatic melanoma. *N Engl J Med* 2010; 363:711–723.
- Johannessen CM, Boehm JS, Kim SY et al. COT drives resistance to RAF inhibition through MAP kinase pathway reactivation. *Nature* 2010;468:968–972.
- Nazarian R, Shi H, Wang Q et al. Melanomas acquire resistance to B-RAF(V600E) inhibition by RTK or N-RAS upregulation. *Nature* 2010;468:973–977.
- Chapman PB, Hauschild A, Robert C et al. Improved survival with vemurafenib in melanoma with BRAF V600E mutation. *N Engl J Med* 2011;364:2507–2516.
- Robert C, Thomas L, Bondarenko I et al. Ipilimumab plus dacarbazine for previously untreated metastatic melanoma. *N Engl J Med* 2011; 364:2517–2526.
- Reya T, Morrison SJ, Clarke MF et al. Stem cells, cancer and cancer stem cells. *Nature* 2001;414:105–111.
- Cho RW, Clarke MF. Recent advances in cancer stem cells. *Curr Opin Genet Dev* 2008;18:48–53.
- Dirks P. Cancer stem cells: Invitation to a second round. *Nature* 2010; 466:40–41.
- Girouard SD, Murphy GF. Melanoma stem cells: Not rare, but well done. *Lab Invest* 2011;91:647–664.
- Fang D, Nguyen TK, Leishear K et al. A tumorigenic subpopulation with stem cell properties in melanomas. *Cancer Res* 2005;65: 9328–9337.
- Monzani E, Facchetti F, Galmozzi E et al. Melanoma contains CD133 and ABCG2 positive cells with enhanced tumorigenic potential. *Eur J Cancer* 2007;43:935–946.
- Schatten T, Murphy GF, Frank NY et al. Identification of cells initiating human melanomas. *Nature* 2008;451:345–349.
- Keshet GI, Goldstein I, Itzhaki O et al. MDR1 expression identifies human melanoma stem cells. *Biochem Biophys Res Commun* 2008; 368:930–936.
- Boiko AD, Razorenova OV, van de Rijn M et al. Human melanoma-initiating cells express neural crest nerve growth factor receptor CD271. *Nature* 2010;466:133–137.
- Civenni G, Walter A, Kobert N et al. Human CD271-positive melanoma stem cells associated with metastasis establish tumor heterogeneity and long-term growth. *Cancer Res* 2011;71:3098–3109.
- Boonyaratankornkit JB, Yue L, Strachan LR et al. Selection of tumorigenic melanoma cells using ALDH. *J Invest Dermatol* 2010; 130:2799–2808.
- Quintana E, Shackleton M, Sabel MS et al. Efficient tumour formation by single human melanoma cells. *Nature* 2008;456:593–598.
- Quintana E, Shackleton M, Foster HR et al. Phenotypic heterogeneity among tumorigenic melanoma cells from patients that is reversible and not hierarchically organized. *Cancer Cell* 2010;18:510–523.
- Jiang J, Hui CC. Hedgehog signaling in development and cancer. *Dev Cell* 2008;15:801–812.
- Stecca B, Ruiz i Altaba A. Context-dependent regulation of the GLI code in cancer by HEDGEHOG and non-HEDGEHOG signals. *J Mol Cell Biol* 2010;2:84–95.
- Calloni GW, Glavieux-Pardanaud C, Le Douarin NM et al. Sonic Hedgehog promotes the development of multipotent neural crest progenitors endowed with both mesenchymal and neural potentials. *Proc Natl Acad Sci USA* 2007;104:19879–19884.
- Stecca B, Mas C, Clement V et al. Melanomas require HEDGEHOG-GLI signaling regulated by interactions between GLI1 and the RAS-MEK/AKT pathways. *Proc Natl Acad Sci USA* 2007;104:5895–5900.
- Lai K, Kaspar BK, Gage FH et al. Sonic hedgehog regulates adult neural progenitor proliferation in vitro and in vivo. *Nat Neurosci* 2003;6:21–27.



- 28 Machold R, Hayashi S, Rutlin M et al. Sonic hedgehog is required for progenitor cell maintenance in telencephalic stem cell niches. *Neuron* 2003;39:937–950.
- 29 Palma V, Ruiz i Altaba A. Hedgehog-Gli signaling regulates the behavior of cells with stem cell properties in the developing neocortex. *Development* 2004;131:337–345.
- 30 Ahn S, Joyner AL. In vivo analysis of quiescent adult neural stem cells responding to Sonic hedgehog. *Nature* 2005;437:894–897.
- 31 Hutchin ME, Kariapper MS, Grachtchouk M et al. Sustained Hedgehog signaling is required for basal cell carcinoma proliferation and survival: Conditional skin tumorigenesis recapitulates the hair growth cycle. *Genes Dev* 2005;19:214–223.
- 32 Brownell I, Guevara E, Bai CB et al. Nerve-derived sonic hedgehog defines a niche for hair follicle stem cells capable of becoming epidermal stem cells. *Cell Stem Cell* 2011;8:552–565.
- 33 Teglund S, Toftgård R. Hedgehog beyond medulloblastoma and basal cell carcinoma. *Biochim Biophys Acta* 2010;1805:181–208.
- 34 Alexaki VI, Javelaud D, Van Kempen LC et al. GLI2-mediated melanoma invasion and metastasis. *J Natl Cancer Inst* 2010;102:1148–1159.
- 35 Clement V, Sanchez P, de Tribolet N et al. HEDGEHOG-GLI1 signaling regulates human glioma growth, cancer stem cell self-renewal and tumorigenicity. *Curr Biol* 2007;17:165–172.
- 36 Varnat F, Duquet A, Malerba M et al. Human colon cancer epithelial cells harbour active HEDGEHOG-GLI signaling that is essential for tumour growth, recurrence, metastasis and stem cell survival and expansion. *EMBO Mol Med* 2009;1:338–351.
- 37 Song Z, Yue W, Wei B et al. Sonic hedgehog pathway is essential for maintenance of cancer stem-like cells in human gastric cancer. *PLoS One* 2011;6:e17687.
- 38 Peacock CD, Wang Q, Gesell GS et al. Hedgehog signaling maintains a tumor stem cell compartment in multiple myeloma. *Proc Natl Acad Sci USA* 2007;104:4048–4053.
- 39 Dierks C, Beigi R, Guo GR et al. Expansion of Bcr-Abl-positive leukemic stem cells is dependent on Hedgehog pathway activation. *Cancer Cell* 2008;4:238–249.
- 40 Prasmickaite L, Engesaeter BØ, Skrbø N et al. Aldehyde dehydrogenase (ALDH) activity does not select for cells with enhanced aggressive properties in malignant melanoma. *PLoS One* 2010;5:e10731.
- 41 Stecca B, Ruiz i Altaba A. A GLI1-p53 inhibitory loop controls neural stem cell and tumour cell numbers. *EMBO J* 2009;28:663–676.
- 42 Taipale J, Chen JK, Cooper MK et al. Effects of oncogenic mutations in smoothened and patched can be reversed by cyclopamine. *Nature* 2000;406:1005–1009.
- 43 Lauth M, Bergström A, Shimokawa T et al. Inhibition of GLI-mediated transcription and tumor cell growth by small-molecule antagonists. *Proc Natl Acad Sci USA* 2007;104:8455–8460.
- 44 Ginestier C, Hur MH, Charafe-Jauffret E et al. ALDH1 is a marker of normal and malignant human mammary stem cells and a predictor of poor clinical outcome. *Cell Stem Cell* 2007;1:555–567.
- 45 Perego M, Tortoreto M, Tragni G et al. Heterogeneous phenotype of human cells with *in vitro* and *in vivo* features of tumor-initiating cells. *J Invest Dermatol* 2010;130:1877–1886.
- 46 Huang EH, Hynes MJ, Zhang T et al. Aldehyde dehydrogenase 1 is marker for normal and malignant human colonic stem cells (SC) and tracks SC overpopulation during colon tumorigenesis. *Cancer Res* 2009;69:3382–3389.
- 47 Sullivan JP, Spinola M, Dodge M et al. Aldehyde dehydrogenase activity selects for lung adenocarcinoma stem cells dependent on notch signaling. *Cancer Res* 2010;70:9937–9948.
- 48 van den Hoogen C, van der Horst G, Cheung H et al. High aldehyde dehydrogenase activity identifies tumor-initiating and metastasis-initiating cells in human prostate cancer. *Cancer Res* 2010;70:5163–5173.
- 49 Cheung C, Davies NG, Hoog JO et al. Species variations in cutaneous alcohol dehydrogenase and aldehyde dehydrogenases may impact on toxicological assessments of alcohols and aldehydes. *Toxicology* 2003;184:97–112.
- 50 Lee J, Platt KA, Censullo P et al. Gli1 is a target of Sonic hedgehog that induces ventral neural tube development. *Development* 1997;124:2537–2552.
- 51 Kasper M, Schnidar H, Neill GW et al. Selective modulation of Hedgehog/Gli target gene expression by epidermal growth factor signaling in human keratinocytes. *Mol Cell Biol* 2006;26:6283–6298.
- 52 Dennler S, André J, Alexaki I et al. Induction of sonic hedgehog mediators by transforming growth factor-beta: Smad3-dependent activation of Gli2 and Gli1 expression in vitro and in vivo. *Cancer Res* 2007;67:6981–6986.
- 53 Nolan-Stevaux O, Lau J, Truitt ML et al. GLI1 is regulated through Smoothened-independent mechanisms in neoplastic pancreatic ducts and mediates PDAC cell survival and transformation. *Genes Dev* 2009;23:24–36.
- 54 Eberl M, Klingler S, Mangelberger D et al. Hedgehog-EGFR cooperation response genes determine the oncogenic phenotype of basal cell carcinoma and tumour-initiating pancreatic cancer cells. *EMBO Mol Med* 2012;4:218–233.
- 55 Keeler RF. Cyclopamine and related steroidal alkaloid teratogens: Their occurrence, structural relationship, and biologic effects. *Lipids* 1978;13:708–715.
- 56 Cooper MK, Porter JA, Young KE et al. Teratogen-mediated inhibition of target tissue response to Shh signaling. *Science* 1998;280:1603–1607.
- 57 Incardona JP, Gaffield W, Kapur RP et al. The teratogenic Veratrum alkaloid cyclopamine inhibits sonic hedgehog signal transduction. *Development* 1998;125:3553–3562.
- 58 Sanchez P, Hernández AM, Stecca B et al. Inhibition of prostate cancer proliferation by interference with SONIC HEDGEHOG-GLI1 signaling. *Proc Natl Acad Sci USA* 2004;101:12561–12566.
- 59 Desch P, Asslaber D, Kern D et al. Inhibition of GLI, but not smoothened, induces apoptosis in chronic lymphocytic leukemia cells. *Oncogene* 2010;29:4885–4895.
- 60 Mazumdar T, DeVecchio J, Shi T et al. Hedgehog signaling drives cellular survival in human colon carcinoma cells. *Cancer Res* 2011;71:1092–1102.
- 61 Takahashi K, Yamanaka S. Induction of pluripotent stem cells from mouse embryonic and adult fibroblast cultures by defined factors. *Cell* 2006;126:663–676.
- 62 Ramgolam K, Lauriol J, Lalou C et al. Melanoma spheroids grown under neural crest cell conditions are highly plastic migratory/invasive tumor cells endowed with immunomodulator function. *PLoS One* 2011;6:e18784.
- 63 Hendrix MJ, Seftor EA, Seftor RE et al. Reprogramming metastatic tumour cells with embryonic microenvironments. *Nat Rev Cancer* 2007;7:246–255.
- 64 Schatton T, Frank MH. Cancer stem cells and human malignant melanoma. *Pigment Cell Melanoma Res* 2008;21:39–55.
- 65 Roesch A, Fukunaga-Kalabis M, Schmidt EC et al. A temporary distinct subpopulation of slow-cycling melanoma cells is required for continuous tumor growth. *Cell* 2010;141:583–594.
- 66 Cheli Y, Guiliano S, Botton T et al. Mif1 is the key molecular switch between mouse of human melanoma initiating cells and their differentiated progeny. *Oncogene* 2011;30:2307–2318.
- 67 Croker AK, Allan AL. Inhibition of aldehyde dehydrogenase (ALDH) activity reduces chemotherapy and radiation resistance of stem-like ALDH(hi)CD44 (+) human breast cancer cells. *Breast Cancer Res Treat* 2011;133:75–87.



See [www.StemCells.com](http://www.StemCells.com) for supporting information available online.